R B Jeyapradha[1,*],
V Rajini[2],
S Gayathri[3]

J. Electrical Systems 20-2 (2024): 181-193

Regular paper

Control Design and Optimization of Magnetics in BIFRED Converter

Journal of Electrical Systems

Non-linear loads being ubiquitous in electrical systems demand modern power factor correction (PFC) techniques. Research related to power factor correction methods in power electronic converters have resulted in integration of converter topologies with single stage power conversion involving a single switch. One such integrated topology is the Boost Integrated Flyback Rectifier Energy DC-DC (BIFRED) converter. This paper compares two current-mode control techniques namely, average current-mode (ACM) control and peak current-mode (PCM) control as applicable to BIFRED converter. Simulation case studies are presented and the performance of the converter with ACM and PCM control are discussed. Further, the magnetic elements of the BIFRED converter are optimized for better performance of the converter. The optimization method followed is based on core geometry coefficient recently published in literature. Experimental hardware of BIFRED converter with average current-mode control and optimized magnetics is developed and the results are illustrated to establish satisfactory performance of the converter.

Keywords: Current-mode control; BIFRED converter; power factor correction; flyback transformer; optimization.

1. Introduction

Integrated power electronic converters are increasingly becoming the topic of research in the present decade. This is because modern day applications demand highly efficient and compact converters with better voltage regulation, high input power factor, rapid dynamic response and low installation cost. Multiple topologies of integrated converters have been recorded in literature [1-10]. Boost Integrated Flyback Rectifier Energy DC-DC (BIFRED) converter is one among them. BIFRED converter is a single-stage integrated power electronic converter with a topological structure comprising a boost converter followed by a flyback converter [11]. The key advantage behind the integration of two converter topologies is that single-step ac-dc conversion is possible without the need for a common dc bus. The integration also results in a single-switch converter with low implementation cost. Besides, the BIFRED converter has several striking features including extensive output voltage regulation, energy storage, high input power factor, rectification of low harmonic content, simple control and compact structure [12]. The boost inductor of the BIFRED converter is so designed that the supply current stays discontinuous over the complete operational range whereas, the flyback converter is designed to conduct in continuous mode throughout the specified range of load.

A broad overview of literature reveals that only limited research publications are available in BIFRED converters despite their introduction in the early 90s. A passive clamp circuit has been introduced for the BIFRED converter along with a detailed analysis of resonant type snubber for the same [12]. An improved integrated magnetic BIFRED

Corresponding author: Dr. Jeyapradha R B[1], Researcher, EEE Department, SSN College of Engineering, Tamilnadu, India, jeyapradharb@ssn.edu.in
[2], Professor and Head, EEE Department, SSN College of Engineering, Tamilnadu, India
[3], EEE Department, SSN College of Engineering, Tamilnadu, India

topology with high power density and lower voltage stress is presented in [13]. The authors in [14] have recommended the use of pulse train control technique for regulating the output voltage of the BIFRED converter and have supported their endorsement with experimental results. A simple DC ripple voltage suppression scheme for BIFRED converter with a small-sized energy storage capacitor is outlined in [15]. An online UPS system with the BIFRED converter is reported in [16]. The use of BIFRED converter as a front end converter for voltage control and power factor improvement in a BLDC motor drive has been proposed in [17]. A state space averaged model has been derived and a fuzzy controller is designed for the BIFRED converter [18].The BIFRED converter as power factor correction converter for implementing an LED lamp driver has been reported in [19].

The research work mentioned above focused on the topology, modeling, modes of operation and output voltage regulation of the BIFRED converter. Very few research papers on control schemes for the converter were reported. The major focus of those control schemes was to achieve load voltage regulation and thus results pertaining to line current shaping were hardly presented. The boost inductor and flyback transformer being the major components of the BIFRED converter, their choice and design are highly influential in determining the power density and overall performance of the converter. Again, no or little research efforts were made for the choice and design of boost inductor and transformer. Therefore, the goal of this paper is to concentrate on better control schemes for input current shaping besides minimizing the output voltage ripple. Further, efforts to improve the power density of the converter through proper design of boost inductor and transformer are being made.

Two current control schemes namely, average current control and peak current control as applied to BIFRED converter are discussed in this paper. A comparison of performance for both the schemes has been validated through simulation case study. Also, a common optimization procedure based on core geometry [20-21] for both the boost inductor and flyback transformer is presented. A laboratory prototype of the converter with optimal inductor and transformer is developed and the results are recorded for the converter with and without the optimal design.

2. Design Specifications of BIFRED Converter

The circuit schematic of BIFRED converter is shown in Fig. 1. It consists of a diode bridge rectifier, an EMI filter, a boost converter followed by a fly back converter. The design of boost inductor is such that the boost converter operates in discontinuous mode for line current shaping while the fly back converter operates in continuous conduction mode for output voltage regulation. The bulk capacitor C_b is usually large enough for storage requirements, and hence a constant voltage is maintained over a time period under normal operations. Thus the duty cycle can also be considered constant over the same period. The boost converter operating in discontinuous conduction mode (DCM) draws nearly sinusoidal current from the lines for constant duty cycle operation thereby realizing power factors greater than 0.95.

Table 1: Specifications of BIFRED Converter

Power Output, P_o	500 W
Input Voltage, V_{in}	198 V
Output Voltage, V_o	130 V
AC Current ripple	0.2
Switching Frequency	50 kHz

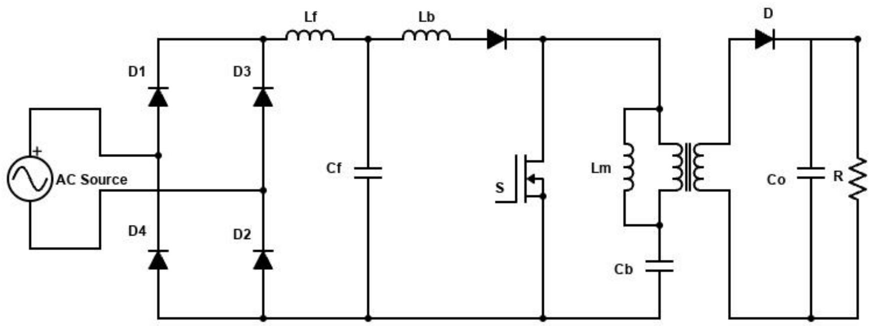

Fig. 1 Basic Schematic of BIFRED Converter

The BIFRED converter has the design specifications listed in Table 1. The design equations of the BIFRED converter are given below [17].

The input voltage V_{in} is given by

$$V_{in} = \frac{2\times\sqrt{2}}{\pi} V_1 = \frac{2\times\sqrt{2}}{\pi} \times 220 = 198 \text{ V} \tag{1}$$

The duty cycle for an output voltage of 130V is given by,

$$D = \frac{n\times V_o}{V_{in}+n \times V_o} = 0.2471 \tag{2}$$

where ‘n’ is the turn’s ratio assumed to be 1:2

The critical value of the boost inductance, L_{cb} for operation in the DCM is given by

$$L_{cb} = \frac{V_{in}\times D}{2 \times f_s \times I_{in}} = 193.74\mu H \tag{3}$$

The value of boost inductance, L_b to operate in DCM is evaluated using

$$L_b < L_{cb} \tag{4}$$

Hence the value of L_b is chosen as 150 µH.

The critical value of the magnetizing inductance, L_m to operate in the boundary between continuous conduction mode (CCM) and DCM is given by

$$L_{cm} = \frac{(1-D)^2}{2\times D\times f_s \times n^2} \times R_L = 3.101 mH \tag{5}$$

The value of magnetising inductance, L_m to operate in DCM is given by

$$L_m < L_{cm} \tag{6}$$

The value of L_m is taken to be around 1/10[th] of L_{mc} to ensure DCM over a wide range of the DC link voltage control. Hence the value of magnetizing inductance is chosen as 350µH.

The bulk capacitor C_b for an allowable ripple voltage, ΔV_{cb} in the bulk capacitor taken as 5% of the peak input voltage is given as

$$C_b = \frac{V_o\times D\times n}{R_L\times f_s \times \Delta V_{cb}} = 930.87 \text{ nF} \tag{7}$$

The value of ouput capacitor, C_o is given by

$$C_o = \frac{I_o}{2 \times \omega_L \times \Delta V_o} = 2354.36\mu F \quad (8)$$

The value of DC link capacitor is thus chosen as 4000 μF (to limit the DC link voltage ripple to less than 2%).The maximum value of the filter capacitance C_{max} is calculated as

$$C_{max} = \frac{I_p}{\omega_L \times V_p} \tan\theta = 574.5nF \quad (9)$$

where I_p is the peak input current, V_p is the peak input voltage and θ is the displacement angle. The value of the filter capacitance, C_f is selected such that C_f is less than C_{max}. Hence the value of C_f is chosen as 330nF.

The filter inductance, L_f is given as

$$L_f = \frac{1}{4\pi^2 \times f_c^2 \times C_f} = 3.07mH \quad (10)$$

where f_c is the cut-off frequency such that f_c=f_s/10.Hence the filter inductance is selected as 4mH.

3. Control of BIFRED Converter

Literature reports two fundamental techniques for the control circuit design of the power converters, namely, voltage-mode and current-mode control techniques. Both the techniques have their own advantages and limitations. The voltage-mode control has a distinctive advantage of single feedback loop which renders easier analysis and design of the circuit topology. Nevertheless, its response to variations in input voltage or load is slower compared to current-mode control [22]. The current-mode control on the other hand is a multi-loop control where the inner loop controls the inductor current, while the outer loop controls output voltage. It offers short-circuit protection and over-current protection in pulse-width modulation (PWM) converters. Also, it exhibits rapid output response and wide-band regulation. Accordingly, it is the most popular technique employed for dc-dc converters. Two current-mode control techniques, viz., average current-mode control and peak current-mode control are designed for the BIFRED converter and their performance compared based on simulation models.

3.1. Average Current-mode (ACM) Control

In this method, the average inductor current is controlled and actively balanced by an RC compensating network. This method is ideally suited for power factor correction circuits as the control reference here is the average current. The control circuit comprises of two parts: current control loop in the feed-forward path and voltage control loop in the feedback path. While the current control loop forces the current waveform to track the shape of the voltage waveform, the voltage control loop along with the gain modulator samples the output voltage and input current respectively. These are then compared to decide if a gain should be applied at the input of current control.

The circuit schematic of ACM control as applied to BIFRED topology is illustrated in Fig. 2.

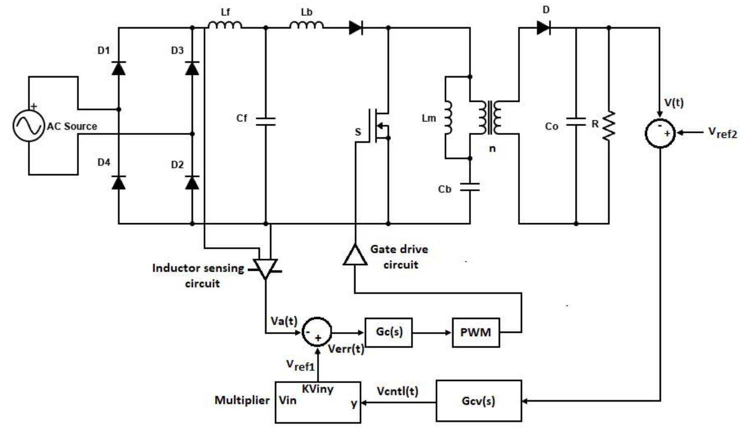

Fig. 2 ACM control of BIFRED Converter

A multiplier block is incorporated in the control circuit for output voltage regulation. The results from the simulation model are presented in Fig.3 to Fig.6. The output voltage from Fig.5 is found to have a ripple of **6.5%.** The Fast Fourier Transform (FFT) analysis of source current represented in Fig. 6 reveals a total harmonic distortion (THD) of **0.41%.**

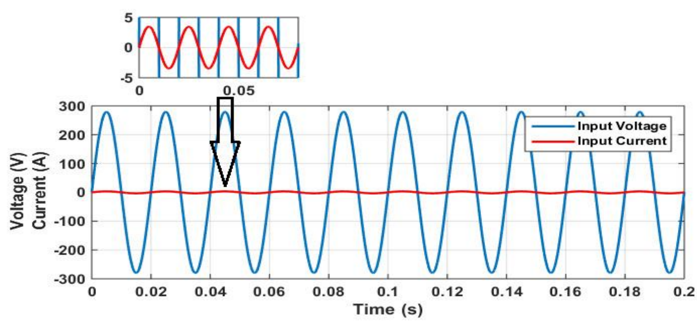

Fig. 3 Source Current and Voltage waveforms of BIFRED converter with ACM control

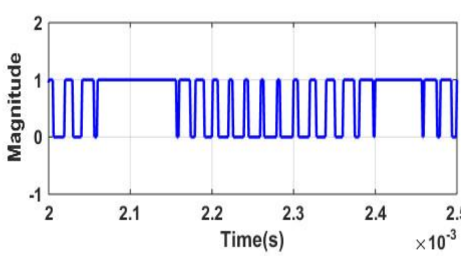

Fig. 4 PWM pulse train to BIFRED converter with ACM control

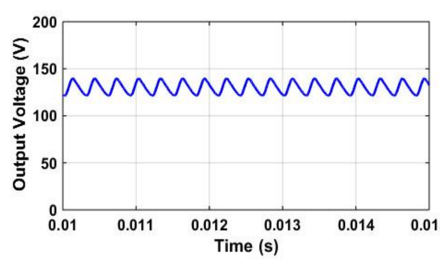

Fig. 5 Output Voltage of BIFRED converter with ACM control

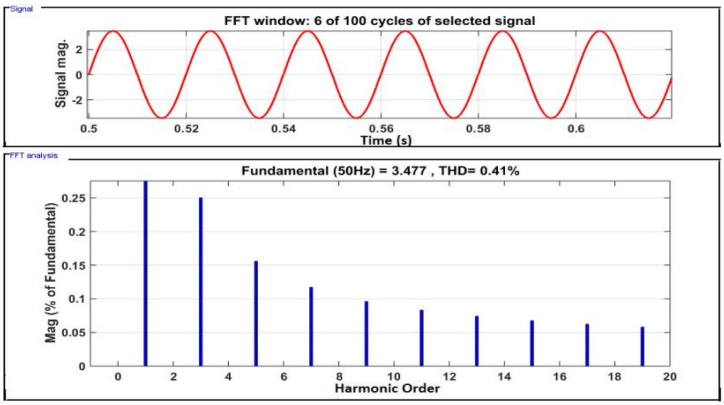

Fig. 6 FFT analysis of Source Current of BIFRED converter with ACM control

3.3. Peak Current-mode (PCM) Control

In this method, the peak current of the inductor is compared with the control current provided by the voltage loop controller. When the inductor current reaches the control current, the device is switched OFF so that the slope of inductor current becomes negative. This mode of control is highly vulnerable to noise thereby resulting in sub-harmonic oscillations due to premature reset of the switch. These oscillations appear at duty cycles above 0.5 and can be removed by addition of an external ramp matching the down-slope of the inductor current to the sensed current.

The circuit schematic of PCM control as applied to BIFRED topology is shown in Fig. 7. The simulation results are depicted in Fig.8 to Fig.11. The output voltage from Fig.10 is found to have a ripple of **2%**. The FFT analysis of source current represented in Fig. 11 reveals a THD of **0.68%.**

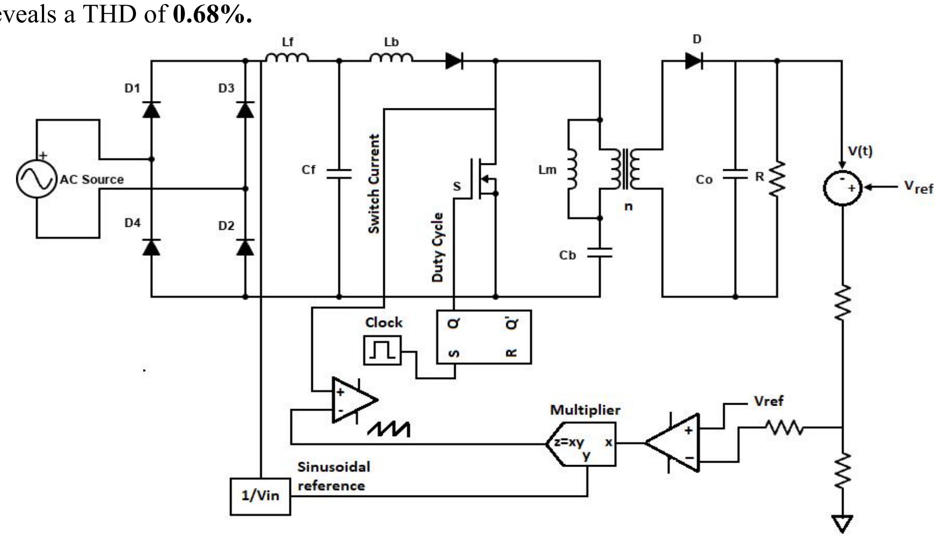

Fig. 7 PCM control of BIFRED Converter

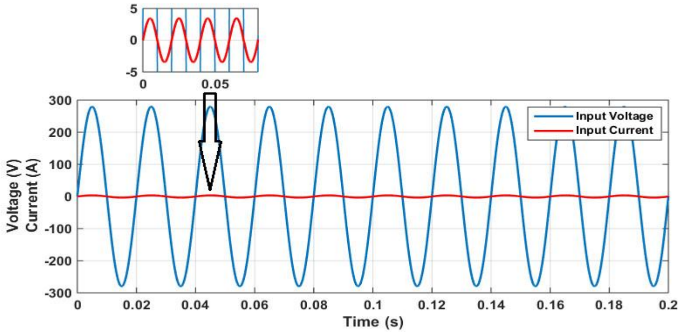

Fig. 8 Source Current and Voltage waveforms of BIFRED converter with PCM control

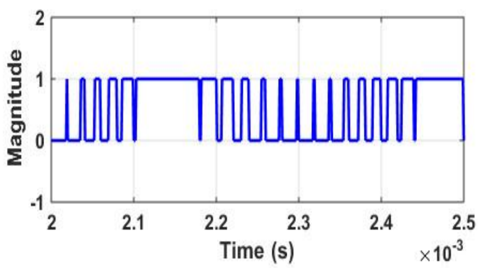

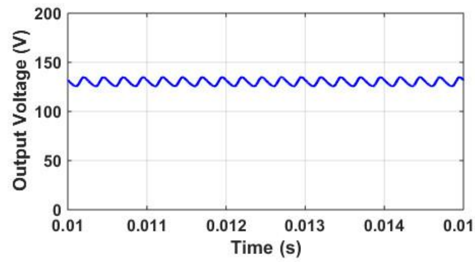

Fig. 9 PWM pulse train to BIFRED converter with PCM control

Fig. 10 Output Voltage of BIFRED converter with PCM control

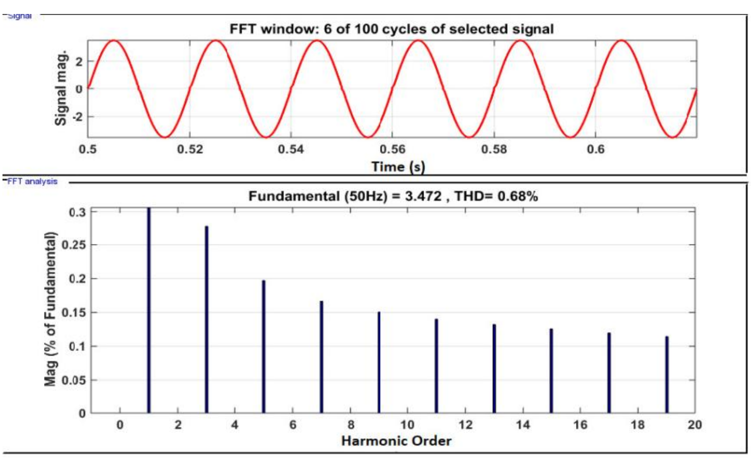

Fig. 11 FFT analysis of Source Current of BIFRED converter with PCM control

The results from the simulation case studies for both the control schemes reveal that the ACM control shows superior performance with respect to power factor correction with a THD of **0.41%** as against **0.68%** for PCM control.

4. Optimization of Magnetics in BIFRED Converter

Besides efficient control design, appropriate choice of boost inductor and flyback transformer is vital to the performance of BIFRED converter. The inductor and transformer being the bulk components of the converter, the power density of the converter are highly influenced by their size and rating. Therefore, this paper focuses on optimizing the magnetics in addition to control design. The optimization procedure followed here is that based on coefficient of core geometry with a constraint on loss density as reported by Banumathy and Veeraraghavalu, 2018. The operating frequency and flux density are chosen as the free parameters. The Particle Swarm Optimization (PSO) algorithm is used for the optimization procedure.

4.1 Optimization of Boost Inductor

The flowchart for optimization of boost inductor is presented in Fig. 12. A total of 105 toroidal core data (from Magnetics Inc.) have been collected including tape wound core, toroidal ferrite core, MPP powder core, Iron powder core and Sendust powder core. The optimization procedure is carried out with a presumed converter efficiency of 96% and a regulation of 0.57%. The optimal values of core geometry, frequency and flux density obtained are listed in Table 2.

Table 2: Optimal Values for Boost Inductor

Coefficient of core geometry	0.00474 cm^5
Frequency	52 kHz
Flux density	0.2 T

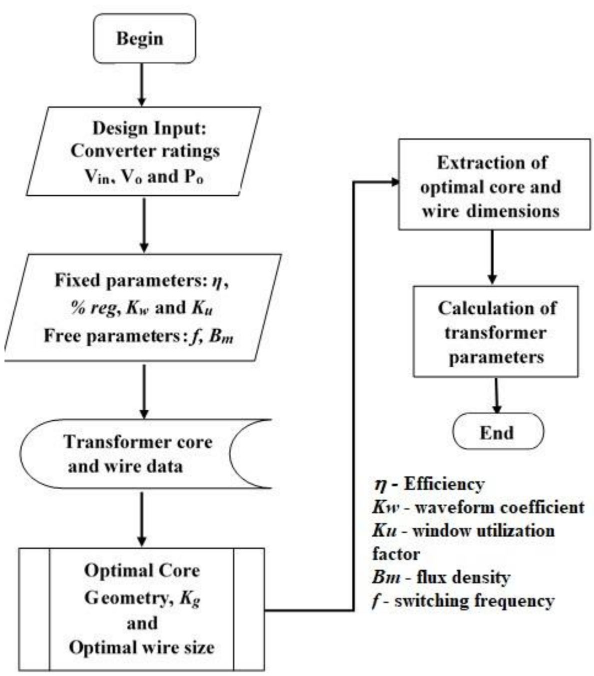

Fig. 12 Flowchart for Boost Inductor Optimization

The core material corresponding to the optimal core geometry coefficient is the MPP toroidal powder core with part no. 55381 and core geometry of 0.005 cm^5.

4.2 Optimization of Flyback Transformer

For optimization of flyback transformer, around 150 cores were considered from the Magnetics manufacturers. The optimization procedure is performed with an assumed converter efficiency of 96% and 0.6 % regulation. The optimal values of core geometry, frequency and flux density obtained are listed in Table 3.

Table 3: Optimal Values for Flyback Transformer

Coefficient of core geometry	0.0110 cm^5
Frequency	51 kHz
Flux density	0.18 T

The core material corresponding to the optimal core geometry coefficient is the EE core with part no. 2425 and core geometry of 0.00957 cm^5.

5. Experimental Hardware and Results

A 200 *W* downscaled BIFRED converter with STM32 controller has been developed with ACM control for validation of results. The converter hardware is presented in Fig.13. The specifications of the hardware and the component ratings are presented in Table 4.

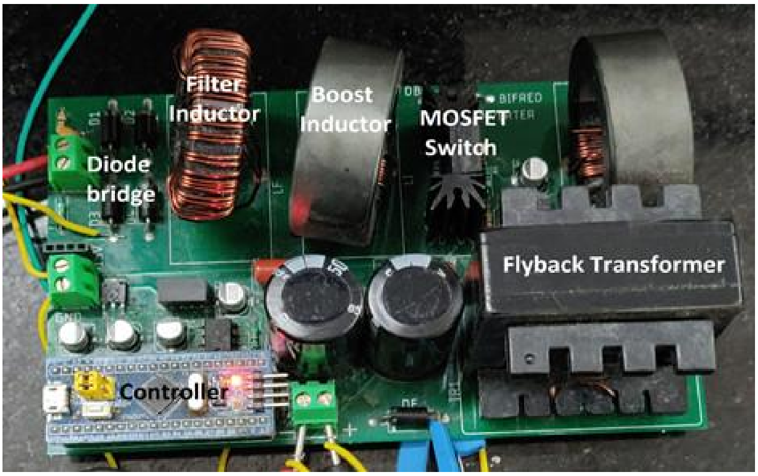

Fig. 13 Experimental hardware of BIFRED Converter

Table 4. Ratings and Specifications of BIFRED Converter

Power rating	200 W
Peak Input Voltage	120 V
Capacitor C_f	200V, 50μF
Diode MUR460	600V 4A
MOSFET	IRF460
Switching Frequency	50 kHz
Inductor L_f	20 mH
Inductor L_1	150 μH
Capacitor C_d	100 μF, 200V
Load	200 W, 18 Ω

The hardware is tested for its performance before and after optimization and the results have been recorded. An input voltage of 120 V peak is applied to the converter and its performance is tested with 200 W, 18 ohms load. The source voltage and current waveforms, output voltage of the diode bridge rectifier, filter inductor current, voltage across the primary and secondary windings of the flyback transformer, switching pulses to the converter and output voltage waveforms of the prototype have been illustrated in Fig. 14 to 25.

Fig.14 to Fig.19 shows the performance of the BIFRED converter without optimization. On the other hand, Fig. 20 to Fig.25 depicts the converter performance with optimized inductor and transformer. It is very much clear from the results that the BIFRED converter shows better performance following optimization. With the optimized magnetics, the source voltage and current waveforms of the BIFRED converter are highly improved as depicted in Fig.20. Also, as can be seen from the primary and secondary voltage waveforms recorded in Fig.23, the flyback transformer exhibits better performance after optimization.

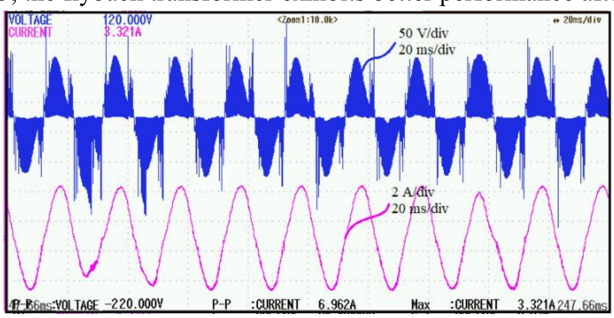

Fig. 14 Source voltage and current of the BIFRED Converter before optimization

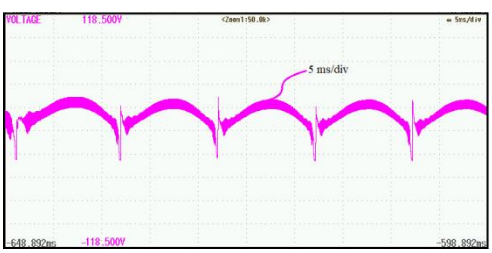

Fig. 15 Output of Bridge rectifier before optimization

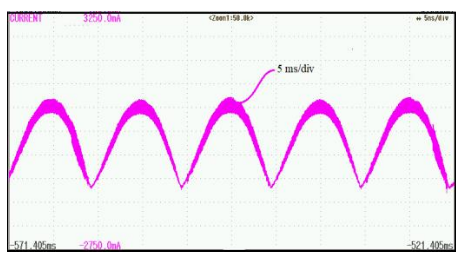

Fig. 16 Current through filter inductor before optimization

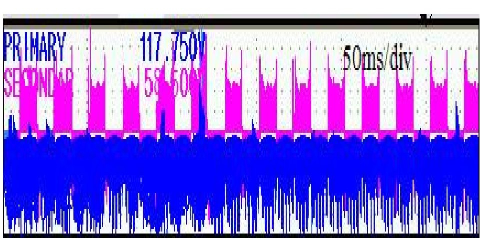

Fig. 17 Primary and secondary voltage of the Flyback transformer before optimization

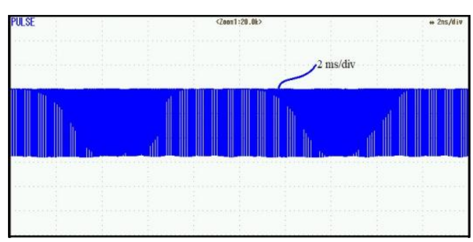

Fig. 18 Switching pulses of the BIFRED Converter before optimization

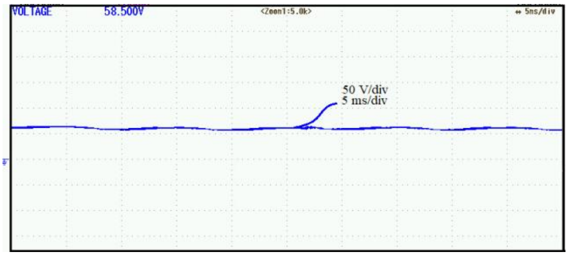

Fig.19 Output voltage of the BIFRED Converter before optimization

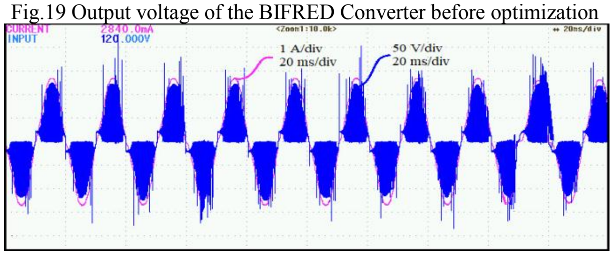

Fig. 20 Source voltage and current of the BIFRED Converter after optimization

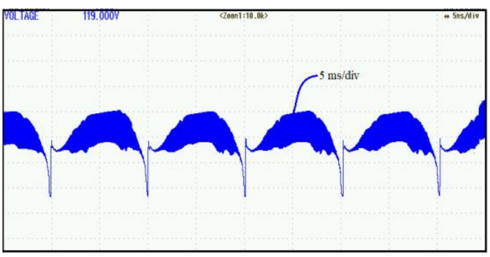

Fig. 21 Output of the Bridge rectifier after optimization

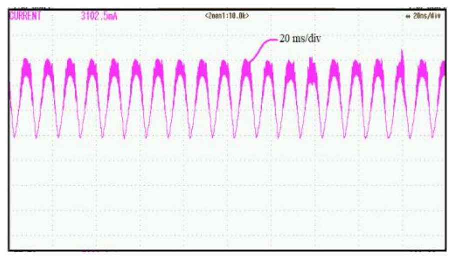

Fig. 22 Filter inductor current after optimization

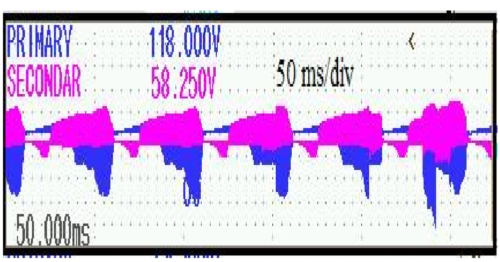

Fig. 23 Primary and secondary voltage of the Flyback transformer after optimization

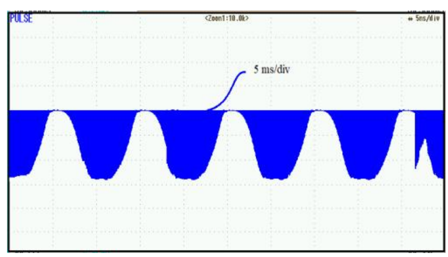

Fig. 24 Switching pulses to the BIFRED Converter after optimization

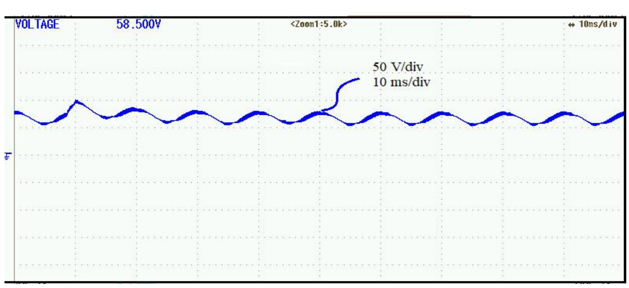

Fig. 25 Output voltage of the BIFRED Converter after optimization

5. Conclusion

This paper was intended to improve the supply power factor of the BIFRED converter through current-mode control techniques. The average current-mode (ACM) control and peak current-mode (PCM) control techniques were applied to BIFRED converter and the performance of the converter was studied. Simulation results showed that the power factor of the converter with ACM control was much better than that of the PCM control. Nevertheless, the output voltage regulation was better with PCM control in comparison to ACM control. Moreover, the boost inductor and isolation transformer of the BIFRED converter were optimized for better performance of the converter. A hardware prototype of the BIFRED converter with ACM control was built with optimized magnetics and the results were presented to approve satisfactory performance of the converter.

Acknowledgment

Authors gratefully acknowledge the SSN Trust for funding this project.

References

[1] A. Khare and K. Anabalagan, A Single-Stage, Multi-Port Hybrid Power Converter Integrating PV and Wind Sources for a Standalone DC System. Energies 2023, 16, 6305

[2] K. Verma, M. Srivastava1, P.S. Tomar, N. Sandeep and A.K. Verma, Single-phase integrated converter with universal battery charging capability for plug-in electric vehicles, *IET Power Electronics,* Vol. 13 No. 4, pp. 821-829, 2020.

[3] G. Ravivarman, A. Amudha, M. Siva Ramkumar and V.M. Mansoor, Single Stage ZVS PFC Circuits with Voltage doubler, *Journal of Electrical Systems,* 17-1 (2021):52-61

[4] R. Uthirasamy, J. Karpagam, V. K.Chinnaiyan,V. J.Vijayalakshmi and P.Ravikumar, Mitigation of Power Quality issues on Hybrid Boost Converter: A Comparative Analysis, *Journal of Electrical Systems,* 16-4 (2020): 478-490

[5] C.-F. Jin and T. Ninomiya, A novel soft-switched single-stage AC-DC converter with low line-current harmonics and low output-voltage ripple, *32nd Annual Power Electronics Specialists Conference*, Vol. 2, (Vancouver, Canada, 2001), pp. 660-665.

[6] C.-W. Roh, G.-W. Moon and M.-J. Youn, Single-stage single-switched rectifier/regulator with magnetic coupled non-dissipative snubber, *Journal of Circuits, Systems and Computers*, 13(3), 557–576, 2004.

[7] G. I. Kishore and R. K. Tripathi, High gain single switched dc-dc converters based on switched capacitors cells, *Journal of Circuits, Systems and Computers* ,29 (12), 2020.

[8] V. Tuomainen, Analysis of three single-stage converters for power factor correction,*Master of Science Thesis*, Helsinki University of Technology, Helsinki, Finland, 1999.

[9] M.T. Madigan, R.W. Erickson and E.H. Ismail, Integrated high-quality rectifier-regulators, *IEEE Trans. Ind. Electron*, 46(4), (1999), 749-758.

[10] T. Oba, H. Murabayashi, S.Murasige and I. Takahashi, Single-switch buck-boost type dither PFC converter, *29th Annual IEEE Power Electronics Specialists Conference*, (Fukuoka, Japan, 1998), pp. 1822-1827.

[11] M. Ferdowsi, Advanced digital control techniques for Integrated power electronic converters, *Doctor of Philosophy Thesis*, Illinois Institute of Technology, Illinois, Chicago, 2004.

[12] V. Tuomainen, Low-power PFC and forward converters –Methods to improve performance, *Doctor of Science in Technology Thesis*, Helsinki University of Technology, Helsinki, Finland, 2002.

[13] A.A. Aboulnaga and A.Emadi, Integrated Magnetic BIFRED Converter with Lower Intermediate Capacitor Voltage, *35th Annul IEEE Power Electronics Specialists Conference*, (Aachen, Germany, 2004), pp. 1551-1556.

[14] M. Ferdowsi, A. Emadi, M. Telefus and A. Shteynberg, Suitability of Pulse Train Control Technique for BIFRED Converter, *IEEE Transactions on Aerospace Electronic Systems*, **41**(1), 181-189, 2005.

[15] J.G. Kim, N.J. Park, D.Y. Lee, D.Y. and D.S. Hyun, A Control Technique for 120Hz DC Output Ripple-Voltage Suppression using BIFRED with a Small-Sized Energy Storage Capacitor, *Journal of Power Electronics*, **5**(3), 190-197, 2005.

[16] A. Nasiri, Z. Nie, S.B. Bekiarov and A. Emadi, An On-Line UPS System With Power Factor Correction and Electric Isolation using BIFRED Converter, *IEEE Transactions on Industrial Electronics*, **55**(2), 722-730, 2008.

[17] B. Singh and V. Bist, Improved power quality IHQRR-BIFRED converter fed BLDC motor drive, *Journal of Power Electronics*, **13**(2), 256-263, 2013.

[18] A. BaharlouHoureh and M.H. Ershadi, Fuzzy Control of BIFRED Converter, *Majlesi Journal of Energy Management*, **8**(1), 13-18, 2019.

[19] M.Z. Efendi, F.D. Murdianto, F.A. Fitri and L. Badriyah, Power factor improvement on LED lamp driver using BIFRED converter, *TELKOMNIKA Telecommunication, Computing, Electronics and Control*, **18**(1), 571-578, 2020.

[20] J.R. Banumathy and R. Veeraraghavalu, High Frequency Transformer Design and Optimization using Bio-inspired Algorithms, *Applied Artificial Intelligence*, **32**(7-8), 1-20, 2018.

[21] J.R. Banumathy and R. Veeraraghavalu, R. Optimal design of Minimal footprint High Frequency Transformer, *Serbian Journal of Electrical Engineering*, Vol. 18 No. 3, pp. 303-320, 2021.

[22] R.M. Kotecha, Analysis and Comparison of Popular Models for Current-Mode Control of Switch Mode Power Supplies, *Master of Science in Engineering Thesis*, Wright State University, Dayton, Ohio, 2010.